We are IntechOpen, the world's leading publisher of Open Access books Built by scientists, for scientists

4,800
Open access books available

122,000
International authors and editors

135M
Downloads

Our authors are among the

154
Countries delivered to

TOP 1%
most cited scientists

12.2%
Contributors from top 500 universities

CLARIVATE ANALYTICS BOOK CITATION INDEX INDEXED

WEB OF SCIENCE™

Selection of our books indexed in the Book Citation Index in Web of Science™ Core Collection (BKCI)

Interested in publishing with us?
Contact book.department@intechopen.com

Numbers displayed above are based on latest data collected.
For more information visit www.intechopen.com

Robot Motion Trajectory-Measurement with Linear Inertial Sensors

Bernard Favre-Bulle

1. Introduction

When referring to the term "industrial robot" in the following, we mean universal, programmable processing machines, which are usually incorporated in industrial manufacturing processes. Industrial robots are multi-functional handling automata which consist of a set of more or less rigid members, interconnected to a kinematic chain by rotational or prismatic joints. One end of this chain represents the base of the robot, the other end is equipped with a tool or a gripper to execute the desired production work. For the considerations presented here (which deal with dynamic trajectory accuracy), we think of both common programming methods, on-line and off-line.

On-line programming usually is based on a teaching-process, where the start- and end-points of a trajectory are defined by moving the robot to the desired poses. An interconnecting trajectory for interpolated movement is then defined by choosing a connective geometry from a library (line, circle, spline-curve) and by specifying additional dynamic parameters as speed or time. Additional "pass-points" can be specified which are not actually a part of the end-effector trajectory but which are passed-by within a certain distance. In point-to-point movements the end-effector does not follow a user-determined path, but is rather defined by the motion of drives in axis-space.

Off-line programming makes use of the known kinematic properties of the robot, the geometrical and structural conditions of the work task and a simulative environment to test the program before implementation on the actual shop-floor. The simulation environment can handle additional tasks like cycle time evaluation, robot cell layout optimization, reach determination, trajectory optimization, simulation and calibration. When a program is transferred from simulation to a real robot station, considerable disparities between simulated and real results can be observed. Deviations of several millimeters can ensue—sufficient to make manufactured parts unusable.

1.1 Robot's Dynamic Errors and Error Measurement

When accurate six-degrees-of-freedom paths with specified maximal errors are required, there is a need for specialized measurement systems for quality assurance and a standard to define a "common language" and information interface between robot manufacturers and robot users. Concerning robot performance characteristics, there is a common standard of evaluating manipulator performance. The International Organization for Standardization (ISO) published the ISO 9283 standard of *Performance Criteria and Related Test Methods* for industrial manipulators. Many robot manufacturers and users utilize this standard to determine the requirements and actual performance of their products and

Source: Cutting Edge Robotics, ISBN 3-86611-038-3, pp. 784, ARS/plV, Germany, July 2005 Edited by: Kordic, V.; Lazinica, A. & Merdan, M.

publish extended specifications based a subset of the tests recommended in ISO 9283. The main points covered in this standard are

- unidirectional pose accuracy and pose repeatability,
- multi-directional pose accuracy variation,
- distance accuracy and distance repeatability,
- pose stabilization time,
- drift of pose characteristics,
- path accuracy and path repeatability,
- cornering deviations,
- path velocity characteristics,
- minimum positioning time and
- static compliance.

Within the scope of the present article, we mainly deal with dynamic performance parameters of the robot motion. Thus, the major criteria to be measured are path accuracy and path repeatability, path velocity characteristics, cornering deviations and pose stabilization characteristics such as swing-over behavior and settling time. There are a lot of sources for deviations between desired and actual robot motion. First of all we have to consider an industrial robot (without external sensors) as a feedback-controlled motion system, which measures kinetic feedback signals at a different location than the task would optimally require, i. e. at the joint drives. The robot's internal sensors usually measure the joint angle positions (and joint velocities, either directly or indirectly) at the drive axes. The joint angles on the robot body are influenced by transmission gear effects (transmission ratios, backlash, elastic deformation of the gears, nonlinear behavior, friction etc.). The robot's mechanical links usually cannot be treated as rigid mechanical elements, since they are elastic and also show a nonlinear mechanical behavior to a certain extent, especially, if high forces are applied to them. Another main source for errors is caused by friction- and backlash-effects within intermediate coupling-elements between the joints and the links. When the motion speed of the robot's links rise, the time dependent interactions between the robots masses, the payload masses and the inertial effects cannot be neglected anymore. At high-speed motion, additional error sources arise from centrifugal and coriolis forces, as well as from mass inertia. All these effects must be taken into consideration for industrial robot calibration. Much research work has been done to achieve an accurate dynamic calibration by means of external sensors (for example Spiess, Vincze et al. 1997, Albada et al. 1996 and Hinüber 1993). Within the presented approach, we utilize inertial sensors, mounted to the robot's end-effector in order to determine its actual dynamic path. We will present a solution to avoid the use of expensive gyroscopic sensors on the basis of a set of linear accelerometers.

1.2 Application of Inertial Measurement Methods

Inertial navigation has a long history (Wrigley, Wrodbary, and Hovorka, I. 1957). The original idea was to utilize inertial effects for the guidance of vehicles (aircraft, spacecraft, missiles, ships etc.). In a historical definition, the guidance process consists of

- measurement of vehicle position and velocity,
- computation of control actions necessary to properly adjust position and velocity, and
- delivery of suitable adjustment commands to the vehicle's control system.

Basically, an inertial guidance system consists of a set of linear accelerometers, e. g. mounted on a gyro-stabilized platform, some kind of computer equipment to perform the inertial calculations and a set of actors to influence the path of the vehicle. A horizontally stabilized platform has the advantage that accelerometer signals can be mathematically integrated within a coordinate system with known orientation relative to the earth's surface, in order to derive speed and actual position of the vehicle. In the first implementations, the platform was stabilized by means of mechanical servo-gyroscopes. Nowadays, these have been replaced by laser-gyros, which show an ever increasing performance. Several new technologies are in development as e. g. an atom interferometer gyroscope, reported in Gustavson, Bouyer and Kasevich (1997), which is based on the Sagnac-effect and which is capable of measuring the earth's rotation rate in a laboratory setup. Systems without stabilized platforms are called "strap-down inertial systems" and have found wide applications in missile systems. They also require gyroscopes, which are comparatively expensive devices for industrial applications. Since one or two decades, inertial navigation systems are also employed for terrestrial vehicles, and thus have found their application for mobile robotics, too.

In aeronautics and spacecraft as well as terrestrial navigation, inertial methods are usually combined with other sources of navigation information. The reason lies in the following fact: Position, orientation, speed and acceleration of the system under measurement must be derived from linear accelerations and angle speeds by multiple integration vs. time. Thus, integrator offset errors and noise contribute to an increasing total position error in time. Starting from an initialization sequence (initial posture of the vehicle, including all temporal derivatives), the inertial measurement system must rely on its high accuracy in order to keep the overall error low. So, the total error rises with operation time (nevertheless, commercial inertial navigation systems for airplanes can keep the total position error as low as a few hundred meters for a 24-hour flight, even without re-calibration and without using other position information).

Concluding, the strength of inertial navigation lies in the short term measurement of highly dynamic motion, as it is the case with industrial robot motion analysis. A proper initialization of the system at the beginning of motion is required, and thus needs at least one other (static) source of navigation information.

2. Inertial Measurement Techniques

Comparing the application properties of inertial vehicle navigation and inertial robot measurement, there are significant differences. In case of robot trajectory analysis, there are

- shorter measurement times,
- shorter absolute path lengths,
- higher accelerations and more acceleration changes per time unit,
- a constant gravity vector along the measurement path and
- easy ways to determine the initial conditions before measurement.

All these circumstances even favor the application of inertial robot path analysis in contrast to vehicle navigation, which on the other hand has proven to be very successful in the past. We are going to recall the basic principles of inertial measurement in the following. From this basis, we will derive a concept for a strap-down inertial measurement platform without gyroscopes. Although low-cost gyroscopic sensors are available on the market today, their application range is limited due to performance parameters. To avoid

the relative high cost for ultra-precision laser gyros, we go for linear accelerometer setups in the present approach.

2.1 Measurement Principles

There are four main system components which are necessary for inertial measurement. We think of a sensor head which is mounted at the end-effector flange (strap-down system) and which contains all necessary components for data acquisition. Categorizing the included devices by their functions, we need

- a sensor system to measure the resulting acceleration vector,
- a device to determine the present orientation in space, relative to the gravity vector,
- a computer system with data acquisition capabilities and
- a real-time clock.

The resulting acceleration vector of the sensor head can be measured by three orthogonally mounted acceleration sensors. The gravity vector needs to be subtracted from the resulting acceleration vector. This procedure requires a) the knowledge of the orientation of gravity, relative to the sensor head orientation and b) the absolute value of gravity acceleration. The orientation of the sensor head can also be determined by a set of accelerometers. After being initialized at the beginning of the measurement process, the actual orientation can be calculated by integrating the angular accelerations twice with respect to time. At initialization time, the gravity vector is known in orientation and size, thus can be tracked and isolated from motion acceleration during rotation of the sensor head.

General motion equation of a rigid body in 3-D space

Let us consider a rigid body with its center of mass **S** which is moved through space by an industrial robot. The motion has six degrees of freedom, and allows each kind of translation and rotation. There is a homogenous acceleration field, induced by the earth's gravity. A rigid body is a system of particles in which the distances between the particles do not vary. To describe the motion of the body we use two different coordinate-systems, a space-fixed system (x_0, y_0, z_0) (vectors with time derivations marked with index *F*) and a moving system (x, y, z) which is rigidly fixed in the body and participates in its motion (vectors with time derivations marked with index *B*). Now let **A** be a point inside the rigid body (see Fig. 1).
With the notation of Fig. 1, we can write down the fundamental motion equation of a rigid body in space with Eq. (1).

$$\ddot{\mathbf{A}}_F = \ddot{\mathbf{R}}_{F,transl.} + \ddot{\mathbf{A}}_B + \dot{\boldsymbol{\omega}} \times \mathbf{A} + 2\boldsymbol{\omega} \times \dot{\mathbf{A}}_B + \boldsymbol{\omega} \times (\boldsymbol{\omega} \times \mathbf{A}) + \mathbf{G} \tag{1}$$

Index *F*	…	time derivations with reference to the space-fixed inertial system
Index *B*	…	time derivations with reference to the body coordinate system
$\ddot{\mathbf{A}}_B$	…	acceleration of point **A** relative to the center of mass **S**
$\ddot{\mathbf{R}}_{F,transl}$	…	translational acceleration of **S**
$\dot{\boldsymbol{\omega}} \times \mathbf{A}$	…	tangential-acceleration
$2\boldsymbol{\omega} \times \dot{\mathbf{A}}_B$	…	coriolis-acceleration
$\boldsymbol{\omega} \times (\boldsymbol{\omega} \times \mathbf{A})$	…	centripetal-acceleration
$\mathbf{G}$	…	vector of gravity

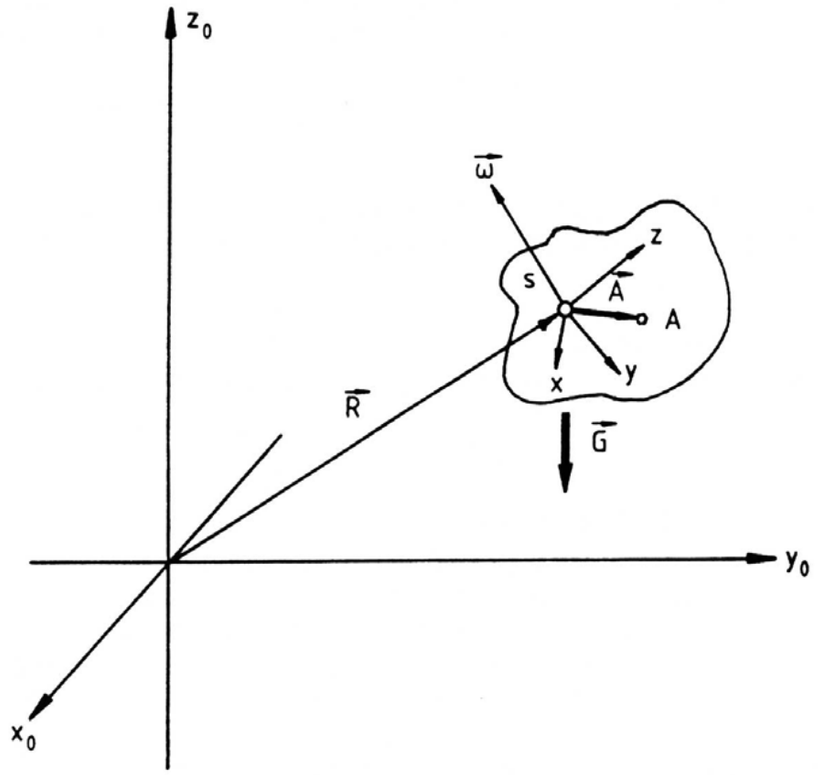

Figure 1. A rigid body in space with six degrees of motion freedom

In case that the point **A** is fixed to the body, the terms $\ddot{\mathbf{A}}_B$ and $2\boldsymbol{\omega}\times\dot{\mathbf{A}}_B$ become zero and we get

$$\ddot{\mathbf{A}}_F = \ddot{\mathbf{R}}_{F,transl.} + \dot{\boldsymbol{\omega}}\times\mathbf{A} + \boldsymbol{\omega}\times(\boldsymbol{\omega}\times\mathbf{A}) + \mathbf{G} \tag{2}$$

The body coordinate system is the coordinate system of the sensor head, and forms the basis for the description of the position and orientation of the accelerometers. To calculate the acceleration $\ddot{\mathbf{A}}_{F,n}$ at the location of the *n*-th accelerometer in the sensor head, we need a coordinate transformation which is determined by the rotation matrix $\mathbf{C}_{F,n}$, thus getting

$$\ddot{\mathbf{A}}_{B,n} = \ddot{\mathbf{A}}_{F,n}\cdot\mathbf{C}_{F,n}. \tag{3}$$

$\mathbf{C}_{F,n}$ contains the Euler-angles $\varphi_x,\varphi_y,\varphi_z$ which describe the orientation of the *n*-th accelerometer in the inertial system. When gravitation influence is present (as it is usual in laboratory environments) we have to take this into account:

$$\ddot{\mathbf{R}}_B = \ddot{\mathbf{R}}_{B,transl.} + \mathbf{G}_B \tag{4}$$

In order to calculate the position and orientation of the sensor head with reference to the fixed-world coordinate system at any time, we have to determine the progression of $\ddot{\mathbf{R}}_B$ and $\boldsymbol{\omega}$ in time from the sensor signals. The number of accelerometers must be at least as high as the number of spatial degrees of freedom.
A system of *i* linear independent acceleration signals in the sensor head leads to a system of *i* equations with variables, consisting of the components of $\ddot{\mathbf{R}}_B$ and $\dot{\boldsymbol{\omega}}$. If the equation

system is solvable, we can isolate $\ddot{\mathbf{R}}_B = \ddot{\mathbf{R}}_{B,transl.} + \mathbf{G}_B$ and $\dot{\boldsymbol{\omega}}$. The actual values of $\varphi_x, \varphi_y, \varphi_z$ at a given time can be determined by integration of $\dot{\boldsymbol{\omega}}$ with respect to time, using $\varphi(0)$ as the integration constant. The gravity influence needs to be compensated by

$$\ddot{\mathbf{R}}_{B,transl.} = \ddot{\mathbf{R}}_B - \mathbf{G}_B, \tag{5}$$

which we will call "auto-compensation" of gravity acceleration (see next paragraph). To get the translational acceleration in fixed world coordinates, we use the direction-cosine matrix **C**

$$\mathbf{C}_{F,B} = \mathbf{C}(\varphi_x, \varphi_y, \varphi_z), \tag{6}$$

and get

$$\ddot{\mathbf{R}}_{F,transl.} = \ddot{\mathbf{R}}_{B,transl.} \cdot \mathbf{C}_{F,B}. \tag{7}$$

$\varphi(t)$ can be calculated from $\dot{\boldsymbol{\omega}}$ by integration. We get $\mathbf{R}(t)$ also by integration:

$$\mathbf{R}(t) = \iint \ddot{\mathbf{R}}_{F,transl.}(t) \; t^2 + \mathbf{R}(0). \tag{8}$$

Auto-compensation of gravity influence

To obtain the pure translatory acceleration component in the sensor head coordinate system, we need to know exactly the amount and orientation of $\mathbf{G}_B(t)$ at each moment. Since $|\mathbf{G}_B(t)| = \text{const.}$ under laboratory conditions, we can calculate $\mathbf{G}_B(t)$ by means of the difference between $(\varphi_x, \varphi_y, \varphi_z)$ and the initial orientation of the sensor head $(\gamma_x, \gamma_y, \gamma_z)$.

$$\mathbf{G}_B(0) = \quad \cdot (1 \quad 1 \quad 1) \; \cdot \mathbf{C}_{(\gamma)}, \tag{9}$$

$$\mathbf{G}_B(t) = \quad \cdot (1 \quad 1 \quad 1) \; \cdot \mathbf{C}_{(\varphi-\gamma)}, \tag{10}$$

with

$_{(\gamma)}$ … direction cosine matrix with the initial angles $\gamma_x, \gamma_y, \gamma_z$

$_{(\varphi-\gamma)}$ … direction cosine matrix with the angle differences $\varphi_x - \gamma_x, \varphi_y - \gamma_y, \varphi_z - \gamma_z$

g … local gravity acceleration (about 9,81 ms^{-2})

Now, we obtain the current values of $\varphi_x, \varphi_y, \varphi_z$ by integration:

$$\varphi(t) = \iint \dot{\boldsymbol{\omega}}(t) \; t^2 + \varphi(0). \tag{11}$$

The auto-compensation of gravity now can be accomplished by finally calculating (5). The process of auto-compensation in gyro - less strap - down systems is very sensitive to any

measurement- and computational errors, since the double integration of $\ddot{\mathbf{R}}(t)$ and $\dot{\boldsymbol{\omega}}$ propagate progressively in time, and the magnitude of the gravity vector may be in the same order of magnitude as the motion accelerations of the sensor head.

2.2 Error Influences

Inertial Navigation Systems ("INS") are intrinsically exposed to a series of error influences. Since the operation principle of each type of INS is based on the integration of signals over time, the total measurement error grows with progression of time.
Schröder-Brzosniowsky (1969) divides the major sources of error in conventional strap-down systems for aeronautics into several categories. This view is based on INS with mechanical gyroscopes. Replacing mechanical gyros by laser gyroscopes or utilizing INS without gyroscopes avoids the occurrence of certain error categories. In the following list, items marked with one asterisk become obsolete when replacing mechanical gyros with laser gyros. Two asterisks indicate errors which are not present in gyro-less systems.

- Drift of gyroscope**
- Mechanical torque perpendicular to the gyro-axis*
- Alignment Errors of gyro**
- Accelerometer system errors
- Accelerometer alignment errors
- INS alignment errors
- Altimeter system errors (for correction of gravity, coriolis- and centripetal forces)
- Geodesic errors (with respect to gravity compensation)

Influence of gravity

As already outlined in the previous paragraph, the physical quantity of acceleration is uniform with respect to motion acceleration and gravity. Thus, the gravity influence needs to be compensated by means of additional information in order to gain measurement signals which are only based on motion-induced acceleration. We can write

$$\ddot{\mathbf{R}}_i = \frac{\mathbf{F}_B + \mathbf{F}_G}{m} = \mathbf{A} + \mathbf{g}_i, \tag{12}$$

with

$\ddot{\mathbf{R}}_i$	…	acceleration vector of the seismic mass
m	…	magnitude of seismic mass
$\mathbf{F}_B/m$, A	…	motion-induced acceleration of the seismic mass
$\mathbf{F}_G/m$	…	gravity-induced acceleration of the seismic mass
Index i	…	quantities with respect to a fixed, non-rotating inertial system

In order to compensate gravity, the gravity-induced acceleration vector needs to be known both in magnitude and orientation. Gravity influence is the most dominant source of error in connection with inertial measurement systems for robotic trajectory analysis.

Influence of earth rotation

The earth represents a system which performs complex motion processes within the stellar system. When neglecting its movement around the sun along the ecliptic, the tidal forces induced by the gravity of moon and sun as well as the earth's precession (conical motion

of the earth axis along a circle within 26000 years), the remaining major influence for inertial navigation is the diurnal rotation of the globe with an angle speed of $7{,}3.10^{-5}$ rad/s. The acceleration vector of a mass point in an inertial system can be expressed as

$$\ddot{\mathbf{R}} = \ddot{\mathbf{R}}_r + \dot{\boldsymbol{\omega}} \times \mathbf{R} + 2\boldsymbol{\omega} \times \dot{\mathbf{R}}_r + \boldsymbol{\omega} \times (\boldsymbol{\omega} \times \mathbf{R}) = \mathbf{A} + \quad , \tag{13}$$

where $\boldsymbol{\omega}$ is the rotation vector of the earth. The index i denotes acceleration and speed measured in a fixed inertial system. Index r refers to the rotating coordinate system of the earth (diurnal motion). Note, that only the first and second derivation of $\mathbf{R}$ with respect to time need to be distinguished with these indices.
For robot trajectory analysis, we assume a typical measurement duration of a few seconds, which represents the time it takes for the end-effector to move from the starting point of its trajectory to the endpoint. Under these circumstances, the effects of earth rotation can be neglected, and so Eq. (13) can be simplified to

$$\ddot{\mathbf{R}} = \mathbf{A} + \quad . \tag{14}$$

2.3 A Two-Dimensional Inertial System Model without Gyroscopes

We will clarify the proposed principle of inertial motion analysis by means of a simple two-dimensional example. We discuss a sensor-head, consisting of three linear accelerometers, arranged like in Fig. 2.

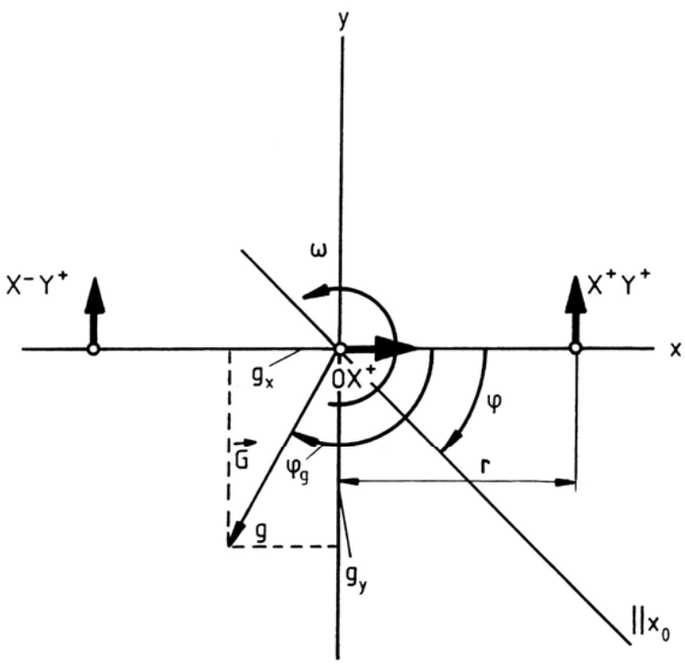

Figure 2. A simple two-dimensional arrangement of three linear accelerometers

The dynamic sensor signals will be denoted as BX^+Y^+, BX^-Y^+ and BOX^+, as indicated by the corresponding arrows in Fig. 2 to show the main sensitivity axes of the accelerometers. The motion-induced acceleration can be split up into two cartesian components b_x and b_y. The parasitic transversal sensitivity of the accelerometers is taken into account with the parameter α. The denotation of variables in equations (15), (16) and (17) are

corresponding to the diagram in Fig. 2. The terms *R* denote random components in the sensor signals, such as noise or thermal offset errors.

$$BX^{+}Y^{+} = b_y + g_y + \alpha\left|b_x + g_x\right| + r\dot{\omega} + \alpha r\omega^2 + R_{X^{+}Y^{+}} \tag{15}$$

$$BX^{-}Y^{+} = b_y + g_y + \alpha\left|b_x + g_x\right| - r\dot{\omega} + \alpha r\omega^2 + R_{X^{-}Y^{+}} \tag{16}$$

$$BOX^{+} = b_x + g_x + \alpha\left|b_y + g_y\right| + R_{OX^{+}} \tag{17}$$

Solving the equation system as explained in paragraph 2.1, we get

$$b_x + g_x = BOX^{+} - R_{OX^{+}} - \alpha/2\left|BX^{-}Y^{+} + BX^{+}Y^{+} - R_{X^{+}Y^{+}} - R_{X^{-}Y^{+}}\right| \tag{18}$$

$$b_y + g_y = 1/2\,(BX^{+}Y^{+} + BX^{-}Y^{+} - R_{X^{+}Y^{+}} - R_{X^{-}Y^{+}}) - \alpha\left|BOX^{+} - R_{BOX^{+}}\right| - \alpha r\omega^2 \tag{19}$$

$$\dot{\omega} = 1/2r\,(BX^{+}Y^{+} - BX^{-}Y^{+} - R_{X^{+}Y^{+}} + R_{X^{-}Y^{+}}) \tag{20}$$

$$\omega = \int\dot{\omega}dt + c(0)\text{ , } c(0) \text{ from initial conditions} \tag{21}$$

The auto-compensation of gravity can be achieved as following:

$$\varphi = \int\omega dt + \varphi(0)\text{ ,} \tag{22}$$

$$\varphi_g = \varphi - \gamma\text{ ,} \tag{23}$$

with γ as initial sensor head orientation,

$$b_x = (b_x + g_x) - |g|\cos\gamma\text{ , and} \tag{24}$$

$$b_y = (b_y + g_y) - |g|\sin\gamma \tag{25}$$

To get the translational accelerations, expressed in coordinates of the fixed inertial system, we need to apply coordinate transformations as following:

$$\begin{pmatrix}\ddot{s}_x\\ \ddot{s}_y\end{pmatrix} = \begin{pmatrix}b_x\\ b_y\end{pmatrix}\begin{pmatrix}\cos\varphi & \sin\varphi\\ \sin\varphi & \cos\varphi\end{pmatrix} \tag{26}$$

The final result of the navigation task is to determine the location of the sensor head by integraton of Eq. (26):

$$s_x(t) = \iint\ddot{s}_x(t)dt + s_x(0)\text{ ,} \tag{27}$$

$$s_y(t) = \iint \ddot{s}_y(t)dt + s_y(0) \tag{28}$$

The discussed calculations are visualized as a block diagram in Fig. 3.

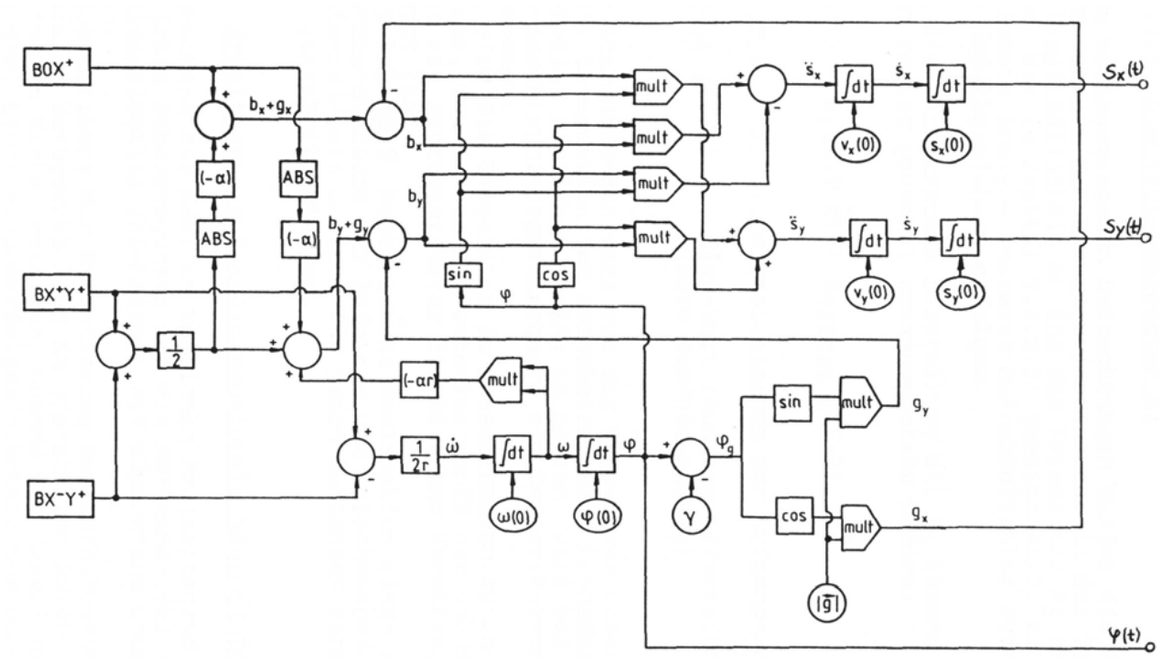

Figure 3. Block diagram for the calculation task with reference to Fig. 2

2.4 Sensors

Industrial acceleration sensors utilize a wide variety of different physical operation principles. We restrict the scope in the present context to *seismic* principles, where the acceleration to be measured exerts a force on a seismic mass. The force is then measured, using different physical effects. The operation principle of spring/mass/damper systems is usually applied in piezo-electric or piezo-resistive transducers. These low-cost sensors types offer a stable performance and a wide application range, but usually don't satisfy the requirements for inertial navigation tasks.

Requirements for inertial navigation accelerometers

Inertial navigation tasks require double integration of acceleration signals to obtain spatial information. This principle imposes specific requirements on the performance parameters of transducers. The following list shows typical requirements, which are fulfilled by the high performance accelerometers series Q-Flex (Honeywell) for aerospace INS:

- Low bias (signal, present at stationary operation at zero gravity without acceleration), typically < 5.10^{-6} g
- Input range +/– 60 g approx.
- Low misalignment (typically < 2000 μrad)
- Low temperature sensitivity on bias (< 20 ppm/°C) and scale factor (< 200 ppm/°C)
- Low cross sensitivity (< 10^{-6} g)
- High linearity (<10^{-5} g/g^2)
- Low intrinsic noise (< 7 μg at 10 Hz, < 1,5 mg at 500–10000 Hz)

High performance accelerometers for inertial navigation purposes are usually designed as servo systems, where a spring-supported seismic mass is held at a mechanical zero position by means of an electromechanical actuator. A control loop is built around the actuator and a position sensor. The closed loop system is kept in balance by force compensation, and the required current to hold the mass in balanced zero position is then proportional to the external acceleration. Fig. 4 shows the model QA3000 from Honeywell for aerospace navigation.

Figure 4. QA3000 Q-Flex® Accelerometer from Honeywell

3. A Three-Dimensional Inertial Sensor Head without Gyroscopes

The principle of gyro-less inertial navigation can be extended for three-dimensional measurement. To analyze trajectories in space (position and orientation), at least 6 accelerometers have to be used. Fig. 5 shows the basic coordinate system for a 3D sensor head.

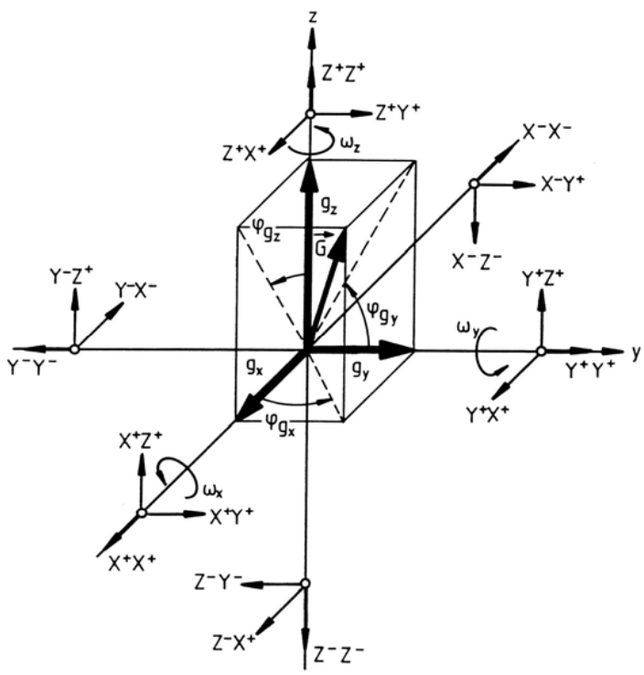

Figure 5. Base coordinate system and accelerometer systems for three-dimensional navigation

An example of a simple accelerometer setup is shown in Fig. 6. The axes of main sensor sensitivity all intersect at the origin of the system. It is easy to understand, how such a setup can measure pure translational accelerations. Changes in orientation of the sensor

head can be sensed by means of the centripetal accelerations. Since these are proportional to ω^2, we can see that the said setup A will be only favorable for high rotation rates. For slow rotations, the centripetal accelerations are very small, which leads to a poor signal/noise ratio.

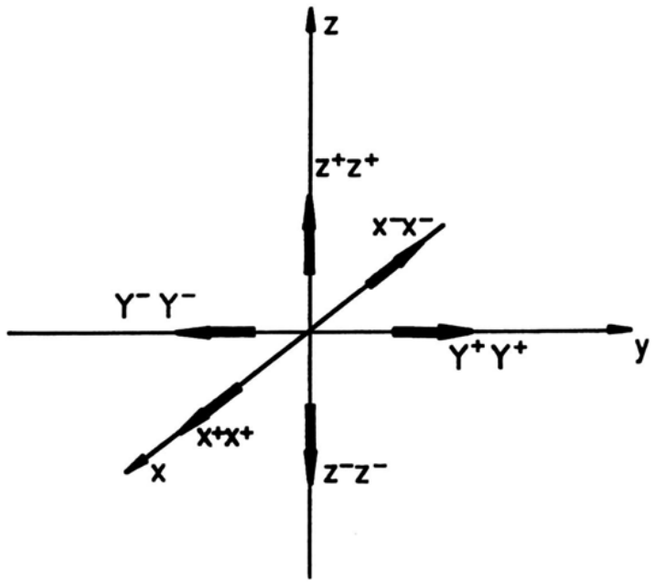

Figure 6. Sensor setup A

To overcome this drawback, one could use a different setup B (Fig. 7). The translational accelerations can be calculated from the average of two corresponding transducers. The orientation change is derived by solving the corresponding equation systems.

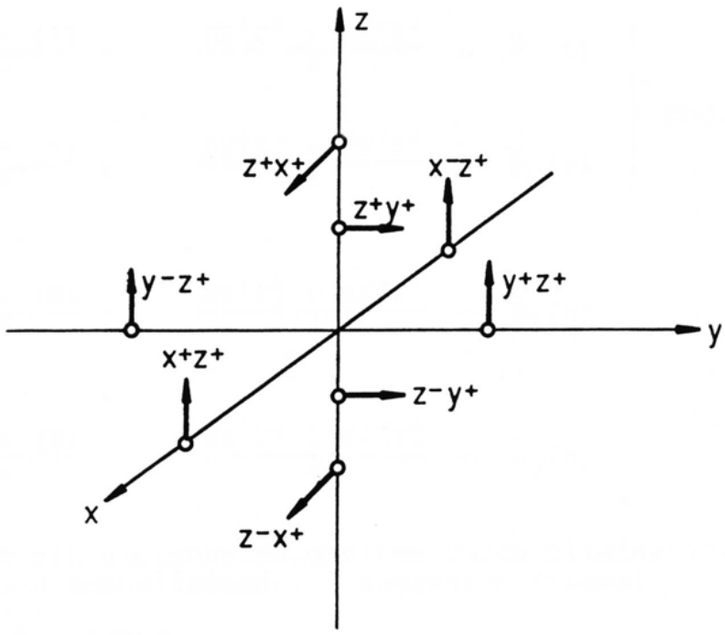

Figure 7. Sensor setup B (using redundancy)

For example, we get

$$\dot{\omega}_x = \frac{BY^+Z^+ - BY^-Z^+ - BZ^+Y^+ + BZ^-Y^+}{-4}, \tag{29}$$

and

$$\omega_z = \frac{BX^+Z^+ - BX^-Z^+ + BZ^+X^+ - BZ^-X^+}{2(\int \dot{\omega}_x(t)dt + \omega_x(0))}. \tag{30}$$

Counting the number of accelerometers in Fig. 7 (eight) we can see, that there is redundancy, i. e., certain kinetic parameters can be determined in different ways. Doing so, one can improve the accuracy of the total measurement result by choosing appropriate accelerometer signals with optimal signal amplitude.

4. Accuracy Improvement by Utilizing Redundant Motion Information

In aeronautical and space applications, INS solutions make use of redundant information to improve the overall accuracy of the position and speed measurement, especially for long-term measurements. The barometric pressure e. g. can be used to estimate the actual distance from the earth's gravity center. The relative airspeed can give an indication of the vehicle speed with respect to the ground, if wind data are available.
Also for robot trajectory analysis with gyro-less strap-down INS, different means of redundancy can be applied to improve overall accuracy of measurements. A few methods and aspects are going to be discussed in the following.

4.1 Utilizing Redundant Accelerometers

As already discussed in the previous paragraph, an increase in the number of accelerometers can improve the overall accuracy.

- Averaging the signals of two corresponding redundant transducers, measuring the *same* quantity can improve signal-to-noise ratio
- Transducers, measuring different quantities at a specific moment (e. g. ω and $\dot{\omega}$) can be selectively chosen on the basis of their current signal magnitude
- Alternative methods can be employed for a more universal approach (Complementary- and Kalman Filters)

Complementary Filters

Higgins (1975) introduces the principle of complementary and Kalman filters and gives a comparison. A complementary filter is used to obtain the estimation of a signal out of two redundant information sources (Fig. 8).
Both signals x and y have their origin in the same information source, although they result from different measurements (e. g. from different transducers). The complementary filter obtains an estimation $\hat{z}$ by filtering the signals through *complementary* networks $1-G(s)$ and $G(s)$. If, for example, signal y is disturbed by high-frequency noise, then it is appropriate to choose a low-pass characteristic for $G(s)$, thus obtaining a high- pass filter

with $1-G(s)$. This should be suitable to suppress low frequency or bias effects within the signal x.

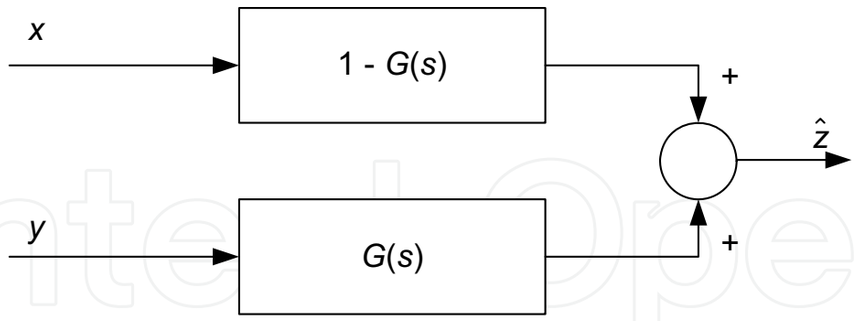

Figure 8. Principle of complementary filters

Kalman Filter

In 1960, R. E. Kalman published a paper describing a recursive solution to the discrete data linear filtering problem. Since that time, the Kalman filter has been subject to extensive investigations. The Kalman filter allows certain predictions within stochastic processes, by separation of noise and signal. It also allows the detection of signals with previously known shape (impulses, sine-waves etc). Fig. 9 shows the application of the filter in inertial measurement tasks. A necessary requirement of successful application is the knowledge of stochastic parameters of the measurement noise (covariance). For further reading, see e. g. Grewal, Weill and Andrews (2000).

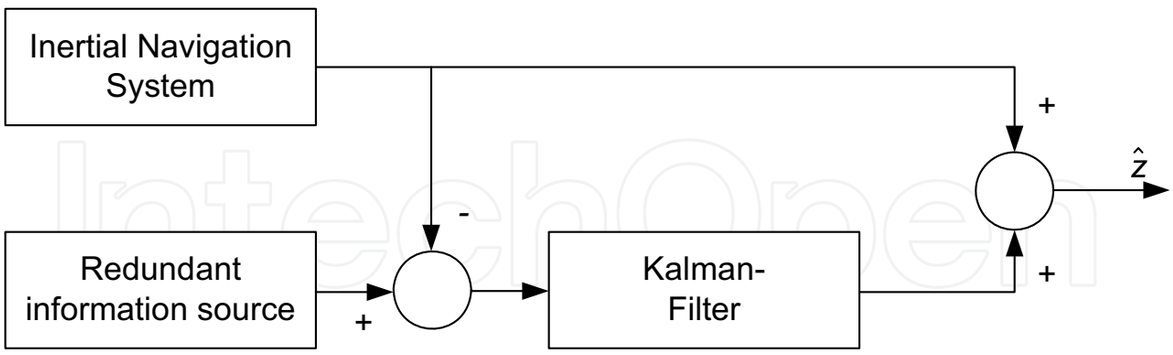

Figure 9. Kalman Filter application in Inertial Navigation

5. Simulation

A simulation with the simple two-dimensional sensor head arrangement from Fig. 2 has been introduced in Favre-Bulle (1993). The goal was to determine influence factors of the sensor head setup and the accelerometer performance parameters on the overall accuracy of the inertial trajectory measurement. A standard two-dimensional motion test pattern has been chosen (Fig. 10).

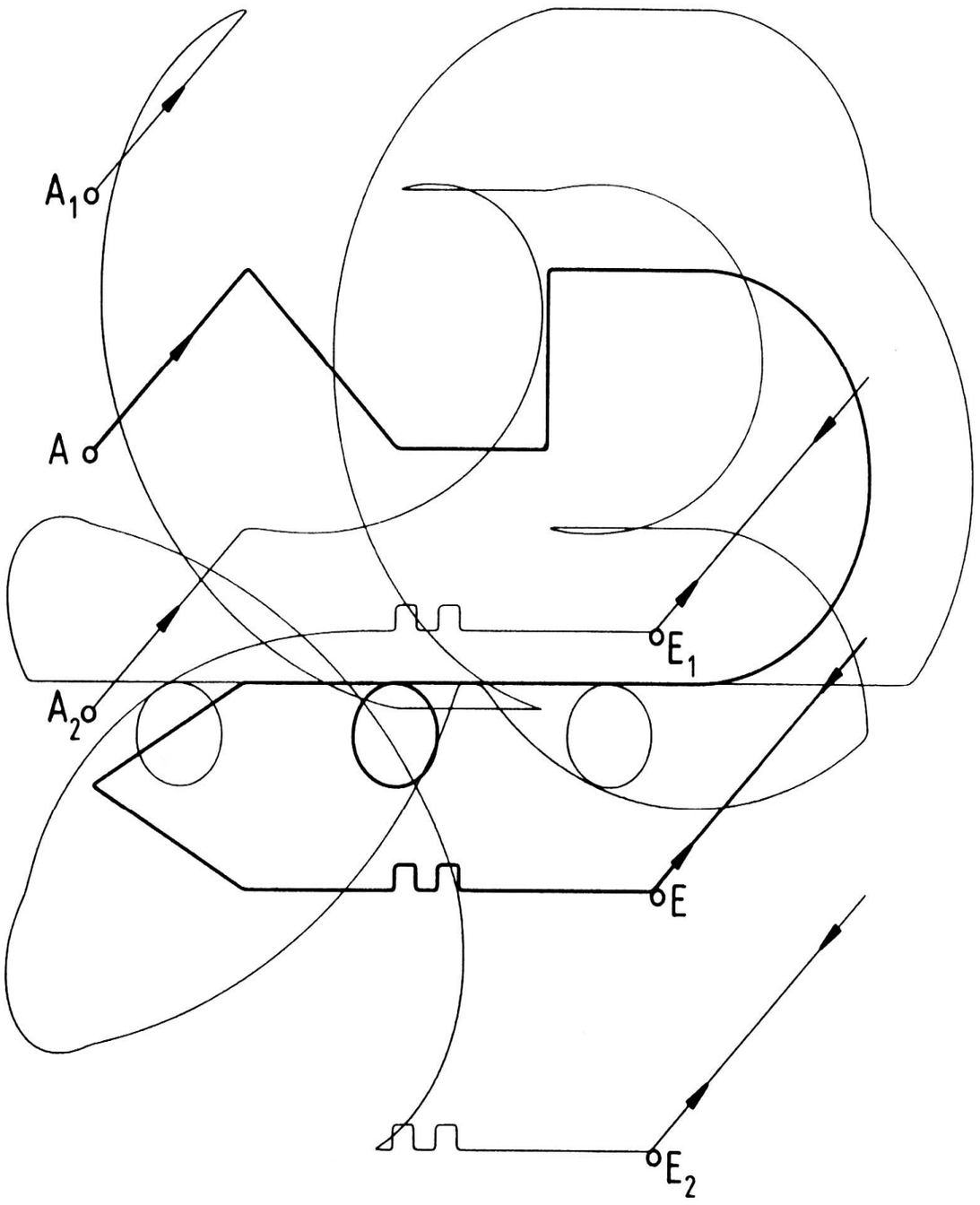

Figure 10. Test pattern for the simulation

This test pattern includes both translation and rotation parts and some combinations of it. Fig. 10 shows the end-effector path in bold line, and the traces of reference points of the three accelerometers. (A to E, A_1 to E_1 and A_2 to E_2).
A dynamic robot model (SCARA-Type) has been established, in order to provide realistic motion behavior of the tool-center-point. Fig. 11 shows the acceleration profiles $\ddot{x}$, $\ddot{y}$ and $\dot{\omega}$ for the first part of the pattern, as they occur at the location of the tool-tip.

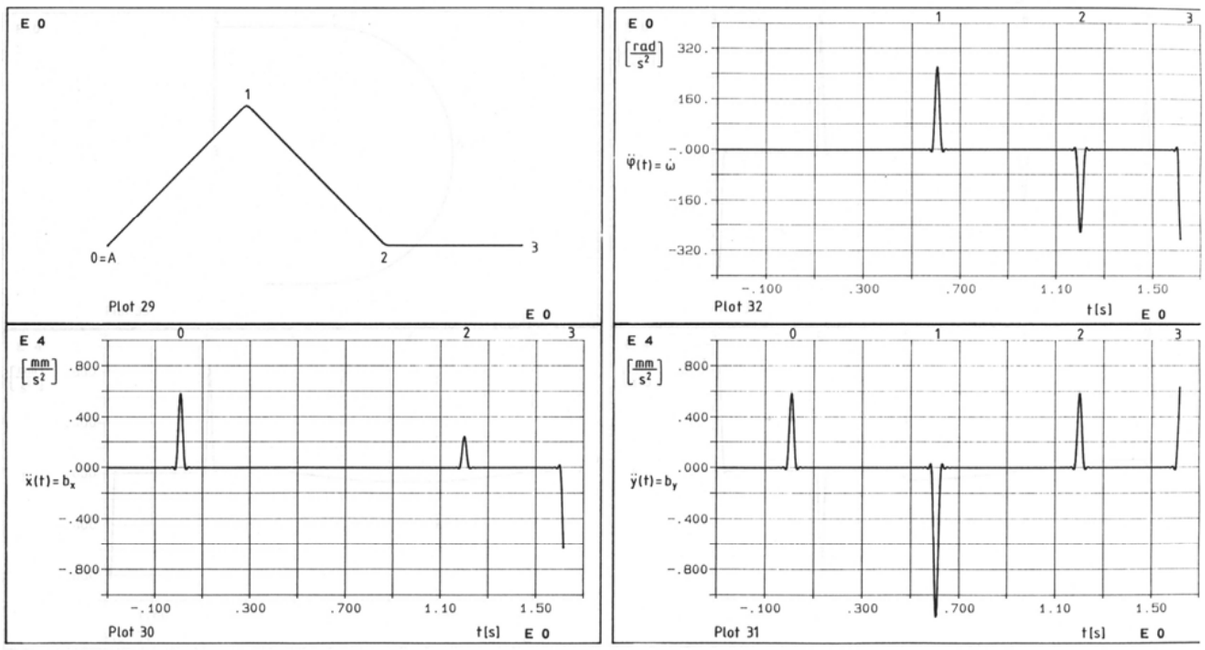

Figure 11. First part of the test trajectory and corresponding acceleration profiles

The linear servo accelerometers in the simulation setup have been modeled with respect to their dynamics, bias-error, scale-error, non-linearities of second and third order, cross-coupling, transversal sensitivity, angle-acceleration sensitivity and misalignment within the sensor head.

Fig. 12 shows the overall measurement error for increasing bias error ($0{,}2.10^{-3}$ g, $0.5.10^{-3}$g and 10^{-3} g) in the accelerometers. These bias errors have been chosen three magnitudes higher than the best possible errors with modern transducers in order to make the resulting effect better visible.

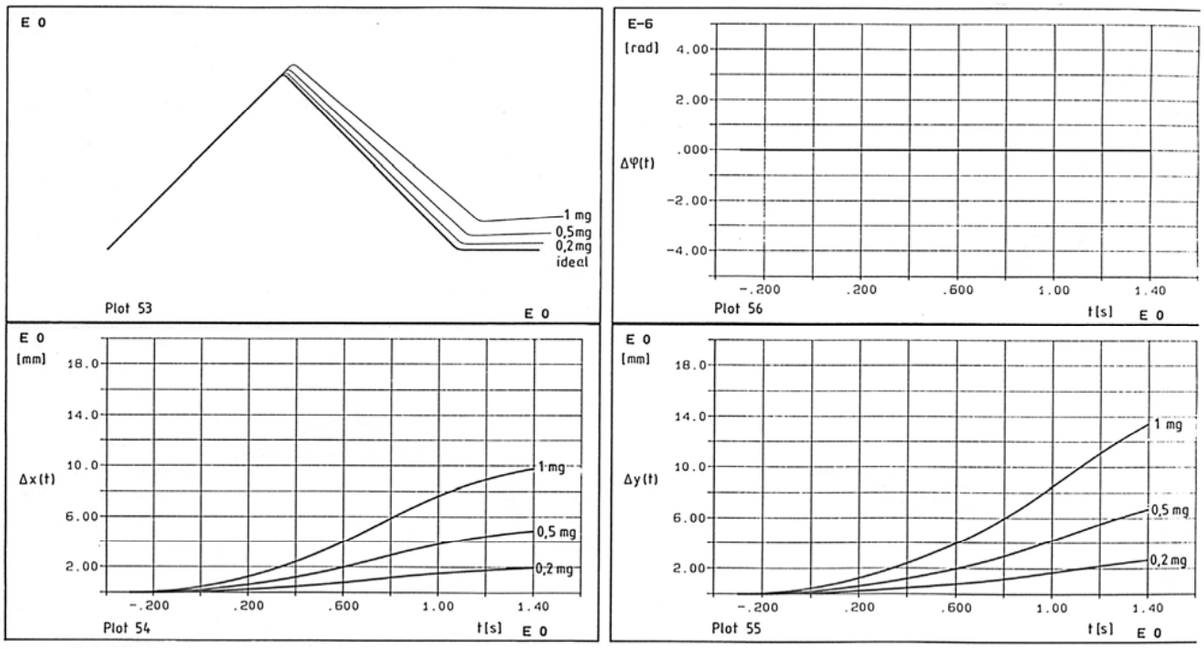

Figure 12. Overall measurement error due to bias errors

Another interesting result is the high sensitivity of the system performance on the angle-acceleration sensitivity of the transducers (Fig. 13).

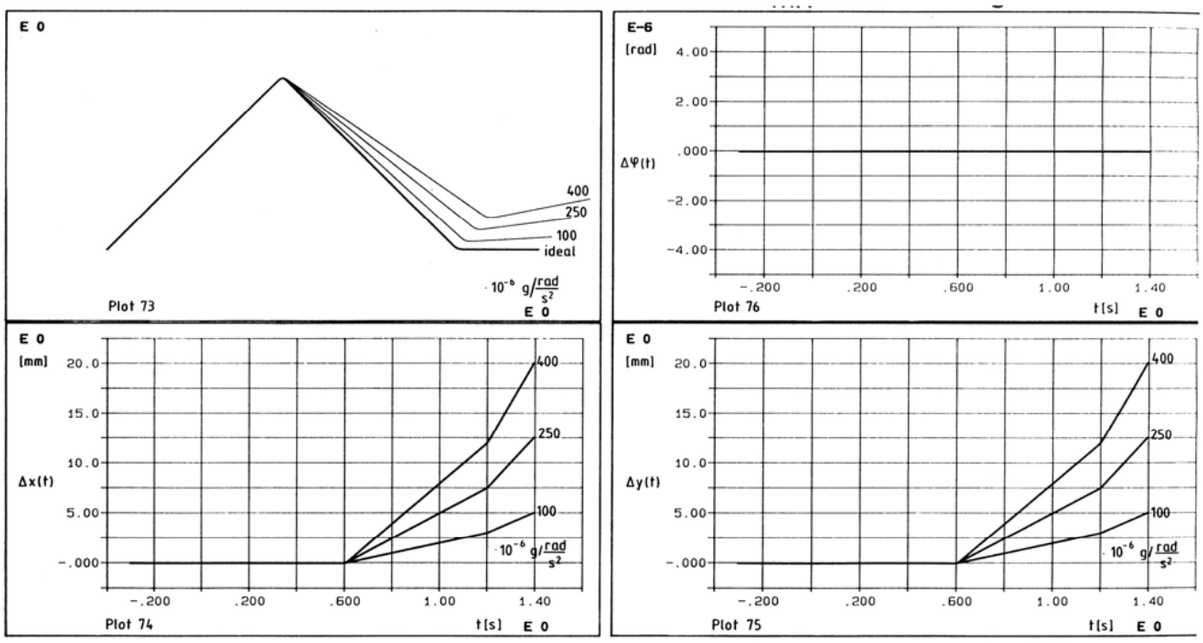

Figure 13. Performance errors of the INS due to angle-acceleration sensitivities

The reason for transducer sensitivity of several accelerometer models with respect to rotational acceleration lies in the fact that the measurement principle uses pendulum-like hinges to support the seismic mass. Thus, not only linear accelerations but also changes in rotation speed cause erroneous behavior.

6. Conclusion

The previous investigations have shown that it is possible to measure dynamic trajectory properties of industrial robots with gyro-less inertial navigation systems. As typical for INS, there are certain sources of errors which distort the overall analysis results to a certain extent. The proposed measurement principle is especially very sensitive to misalignment of the transducers in the sensor head and to bias errors of the accelerometers.

With redundant configurations (e. g. a higher number of transducers than spatial degrees of freedom) there are certain possibilities to improve the overall accuracy by means of complementary filters and Kalman filters.

Further research should investigate the use of low-cost gyroscopes as a source of additional motion information. One interesting "candidate" would be a piezoelectric vibration type gyro, like the Murata Gyrostrar®. Utilizing hybrid, highly-redundant sensor heads made from low-cost components could be a feasible solution for high-accurate trajectory analysis heads for affordable prices.

7. References

Albada, G. D. v., Lagerberg, A. and Visser, J. M. (1996) A low-cost pose-measuring system for robot calibration. Tech. Rep. University of Amsterdam, Faculty of Mathematics and Computer Science

Diewald, B. (1995) Über-alles-Kalibrierung von Industrierobotern zur lokalen Minimierung der Posefehler. PhD thesis, Universität des Saarlandes

Favre-Bulle, B. (1993) An Inertial Navigation System for Robot Measurement and Control. In: 2nd IEEE Conference on Control Applications, Sept. 13–16, Vancouver, B. C.

Grewal, M. S., Weill, L. R. and Andrews, P. (2000) Global Positioning Systems, Inertial Navigation, and Integration. Control Systems Technology & Automation. Wiley

Gustavson, T. L., Bouyer, P. and Kasevich M. A. (1997) Precision Rotation Measurements with an Atom Interferometer Gyroscope. Physical Review Letters, vol. 78 (11), pp. 2046–2049, Department of Physics, Stanford University, Stanford, California

Higgins, W., T. (1975) A Comparison of Complementary and Kalman Filtering. In: IEEE Transactions on Aerospace and Electronic Systems, Vol. AES–11, No. 3, pp. 321–325

Hinüber, E. v. (1993), Bahn- und Positionsvermessung von Industrierobotern mit inertialen Meßsystemen. PhD thesis, Universität des Saarlandes

Hinüber, E. v. and Janocha, H. (1993) Inertial Measurement System for Calibration and Control of Robots. In: Industrial Robots, Vol. 20 No. 2 (1993) pp. 20–27

ISO 9283 (1993) Manipulating Industrial Robots—Performance Criteria and Related Test Methods. International Standardisation Organisation

Janocha, H. and Hinüber, E. v. (1995) Leistungspotential moderner inertialer Meßsysteme. In: ATZ – Automobiltechn. Zeitschr., 97 (1995) , 1, 30–35

Leigh-Lancaster, C. J., Shirinzadeh and B. Koh, Y. L. (1997) Development of a Laser Tracking System. 4th Annual Conference on Mechatronics and Machine Vision in Practice (M2VIP '97), Sept. 23–09, 1997, Toowoomba, Australia

Roos, E., Behrens, A., Anton, S. (1997) RDS—realistic dynamic simulation of robots. In: 28th International Symposium on Robotics, Detroit USA

Schröder-Brzosniowsky, J., (1969) Fehleranalyse bei fahrzeugfesten Trägheitsnavigationssystemen. Berlin

Schröer, K., Albright, S. L. and Grethlein, M. (1997) Complete, minimal and model-continuous kinematic models for robot calibration. In: Robotics and Computer-Integrated Manufacturing, vol. 12, no. 1, pp. 73–85

Shirinzadeh, B. (1998) Laser-interferometry-based tracking for dynamic measurements. Industrial Robot: An International Journal, Vol. 25, No. 1, pp. 35–41, 1998.

Spiess, S., Vincze, M. and Ayromlu, M. (1997) On the calibration of a 6-D laser tracking system for contactless, dynamic robot measurements. In: Proceedings of the IEEE Instrumentation & Measurement Technology Conference, IMTC, Ottawa, pp. 1203–1208

Wrigley, W., Wrodbary, R., Hovorka, I. (1957) Inertial Guidance. Preprint Nr. 698, Institute of the Aeronautical Science, New York

Cutting Edge Robotics

Edited by Vedran Kordic, Aleksandar Lazinica and Munir Merdan

ISBN 3-86611-038-3

Hard cover, 784 pages

Publisher Pro Literatur Verlag, Germany

Published online 01, July, 2005

Published in print edition July, 2005

This book is the result of inspirations and contributions from many researchers worldwide. It presents a collection of wide range research results of robotics scientific community. Various aspects of current research in robotics area are explored and discussed. The book begins with researches in robot modelling & design, in which different approaches in kinematical, dynamical and other design issues of mobile robots are discussed. Second chapter deals with various sensor systems, but the major part of the chapter is devoted to robotic vision systems. Chapter III is devoted to robot navigation and presents different navigation architectures. The chapter IV is devoted to research on adaptive and learning systems in mobile robots area. The chapter V speaks about different application areas of multi-robot systems. Other emerging field is discussed in chapter VI - the human- robot interaction. Chapter VII gives a great tutorial on legged robot systems and one research overview on design of a humanoid robot.The different examples of service robots are showed in chapter VIII. Chapter IX is oriented to industrial robots, i.e. robot manipulators. Different mechatronic systems oriented on robotics are explored in the last chapter of the book.

InTech Europe
University Campus STeP Ri
Slavka Krautzeka 83/A
51000 Rijeka, Croatia
Phone: +385 (51) 770 447
Fax: +385 (51) 686 166
www.intechopen.com

InTech China
Unit 405, Office Block, Hotel Equatorial Shanghai
No.65, Yan An Road (West), Shanghai, 200040, China
中国上海市延安西路65号上海国际贵都大饭店办公楼405单元
Phone: +86-21-62489820
Fax: +86-21-62489821

IntechOpen